Journal of Sound and Vibration (2000) **237**(2), 303–318
doi:10.1006/jsvi.2000.3028, available online at http://www.idealibrary.com on IDEAL®

NON-LINEAR RESPONSE OF A POST-BUCKLED BEAM SUBJECTED TO A HARMONIC AXIAL EXCITATION

J.-C. JI†

Department of Mechanical Engineering, Baotou University of Iron and Steel Technology, Baotou, 014010, Inner Mongolia, People's Republic of China

AND

C. H. HANSEN

Department of Mechanical Engineering, The University of Adelaide, South Australia 5005, *Australia*

(*Received* 30 *November* 1999, *and in final form* 29 *March* 2000)

An experimental investigation of the non-linear response of a clamped–sliding post-buckled beam subjected to a harmonic axial load is presented. Two types of resonances are considered: fundamental and subharmonic. The data demonstrate several non-linear phenomena including period-doubling sequence bifurcation, period-three, and chaotic motion. In addition, the effect of damping on the dynamic instability of the post-buckled beam is investigated. The regions of instability and chaotic response are shown for different damping levels. The resulting locus of instability of the periodic solutions in the amplitude–frequency parameter space provides valuable information on the overall dynamic behavior of the system. The qualitative changes can be observed when either the frequency or the amplitude of excitation is varied across a bifurcation curve. The measured data are illustrated through time histories, phase plots, Fourier spectra, and Poincare sections.

1. INTRODUCTION

During the past two or three decades, a large amount of literature has been devoted to post-buckling behavior analysis and dynamic instability of structures. In the fields of structural engineering, mechanisms and robotics, many structural elements under periodic loads can undergo parametric resonance, which may occur over a range of forcing frequencies. The parametrically excited vibrations of beams, plates, shells, arches, and frames have become popular subjects of study. However, most of the previous buckling studies have focused on the buckling or initial post-buckling behavior.

The non-linear vibrations of beams subjected to periodic excitation have been extensively studied (see [1] and references therein). In particular, Tseng and Dugundji [2] experimentally and analytically investigated the non-linear response and chaotic vibration in a fixed–fixed buckled beam. Later, Moon and Holmes [3] presented a study of the most basic model for a buckled beam and found chaotic responses. Holmes and Moon [4], and Moon and Shaw [5] next reported chaotic behavior of a cantilever beam with magnetic attractors at its free end. Subsequently, Moon and Holmes [6] experimentally studied chaotic dynamics of a buckled beam forced with two frequencies. Abhyankar *et al.* [7]

† Author to whom correspondence should be addressed. Department of Building and Construction, City University of Hong Kong, Tat Chee Avenue, Kowloon, Hong Kong. E-mail: jchji2@hotmail.com, bcjjc@cityu.edu.hk

0022-460X/00/420303 + 16 $35.00/0

directly conducted numerical integration of the partial differential equation of a simply supported buckled beam to investigate chaotic vibrations.

The governing equation in most of the previous work is given by the most basic model for a buckled beam, which is Duffing's equation with an external sinusoidal excitation. Abou-Rayan and Nayfeh [8] investigated the non-linear response of a simply supported buckled beam to a harmonic axial load. The physical system was modelled as a parametrically excited Duffing oscillator (two potential wells). They used the method of multiple scales to determine the amplitude- and phase-modulation equations for fundamental and subharmonic resonance, and Floquet theory to analyze the stability of the periodic response. Moreover, analog and digital simulations were used to verify the perturbation results. They found rich non-linear phenomena. To the author's knowledge, the experimental investigation of the non-linear response of a post-buckled beam subjected to a parametric excitation has not been reported previously.

In the context of non-linear oscillations, non-linear parametrically excited oscillators have also been extensively analyzed [1, 9–20]. Chen and Langford [21] used Liapunov–Schmidt reduction [22] and the theory of singularities to develop a C–L method to study subharmonic bifurcation of a generally non-linear Mathieu's system. Sanchez and Nayfeh [23] determined the instability regions of the response of a damped, softening-type Duffing oscillator to a parametric excitation via an algorithm based on Floquet theory. They constructed a bifurcation diagram and found that the periodic solutions lose stability through three types of bifurcation.

In contrast to the extensive theoretical work published on parametrically excited non-linear systems, only limited experiments have been reported in the literature that validate or, at least qualitatively support the theoretical results. Nayfeh *et al.* [24] validated experimentally the analytically obtained natural frequencies and mode shapes for a clamped–clamped first-mode buckled beam. Zavodney and Nayfeh [25] investigated the dynamics of a cantilever beam carrying a lumped mass. They modelled the structure with cubic geometric and inertia non-linearities. They conducted experiments and reported results that were in general agreement with the theoretical predictions. Anderson *et al.* [26] improved the model proposed by Zavodney and Nayfeh [25] and considered the effect of quadratic damping on the response of the system. Their theoretical results agreed with the experimental observations. However, many non-linear phenomena predicted to exist as a part of the overall dynamic behavior of oscillators with parametric excitation are yet to be demonstrated experimentally.

As a consequence, this paper will focus on an experimental study of the non-linear response of a post-buckled beam subjected to a harmonic axial load. The system can be modelled as a non-linear oscillator with parametric excitation. The intent here is not to mathematically describe the complex nature of the entire non-linear system behavior, but to develop a general understanding of the phenomena that may be applied to the many engineering problems that fall in this category.

During the experimental work, decreasing or increasing the normal compressive force on the sliding end will be used to vary the external frictional force, such that the coefficients of the linear and non-linear damping terms in the equation change. Thus, the effect of damping on the dynamic instability of a post-buckled beam will be investigated.

2. EXPERIMENTAL MODEL

A physical model of the investigated beam is depicted in Figure 1. The beam was compressed by an axial load composed of static and harmonic components. In order to

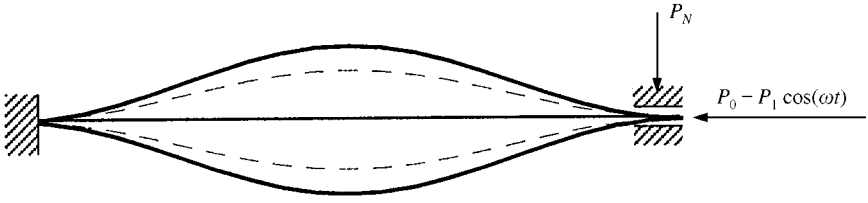

Figure 1. Geometry of the post-buckled beam.

investigate the non-linear response of a post-buckled beam, the static component was set above the first critical load for buckling. A normal force P_N was applied to the beam at the sliding end to control the frictional force at that location. During the experiment, decreasing or increasing the normal compressive force P_N on the sliding end was used to vary the external frictional force. This sort of damping can be represented approximately by a speed-dependent damping function [27, 28]. For a one-mode approximation, the non-dimensional equation of motion is approximated by a degree-of-freedom non-linear oscillator with parametric excitation:

$$\ddot{u} + \mu_0 \dot{u} + \mu_1 \dot{u}^3 + u + \alpha_1 u^2 + \alpha_2 u^3 + fu\cos\Omega t + f\cos\Omega t = 0. \tag{1}$$

More details can be found in reference [29].

3. EXPERIMENTAL APPARATUS AND PROCEDURE

A schematic of the experimental set-up is shown in Figure 2. The test specimen was a uniform beam with rectangular cross-section made of carbon steel. The dimensions of the beam were 535 mm∗31 mm∗1·5 mm. The apparatus consisted of four components: the test specimen, the excitation system, the data acquisition system and the signal processing system. The beam was excited along its axis at its sliding end by a PR9270 vibration exciter driven by a power amplifier and a sinusoidal wave synthesizer. The excitation amplitude was held constant (as the excitation frequency was swept) by a computer-controlled feedback loop.

Two accelerometers mounted on the middle span of the beam were used to pick up the vibration signals proportional to the transverse displacement and velocity of the beam. The signals were monitored by a digital oscilloscope, recorded by a cassette recorder, and sent to an IBM PC that acquired data through a 16-bit analog-to-digital converter. A sampling frequency of 376 Hz was used and 2048 points per set were collected. The acquired data were stored in the IBM PC and directly analyzed by a FFT algorithm.

The linear resonance frequencies of the beam were first determined by using band-limited random excitation, and then the estimates were refined by conducting slow sine sweeps about each frequency value. Of course, the choice of the measurement point depends on the modes involved in the response. The measuring point should be away from nodal points of any of the active modes. The modal testing was performed for different measurement locations along the beam. In this way, the possibility of missing a linear natural frequency because of the measuring point being near a nodal point was reduced. The modal tests were conducted for different forcing levels to ensure that the estimated frequencies did not depend on the vibration amplitude. The first two linear resonance frequencies of the beam were experimentally obtained to be 5·7 and 24·11 Hz. The modal damping coefficients were

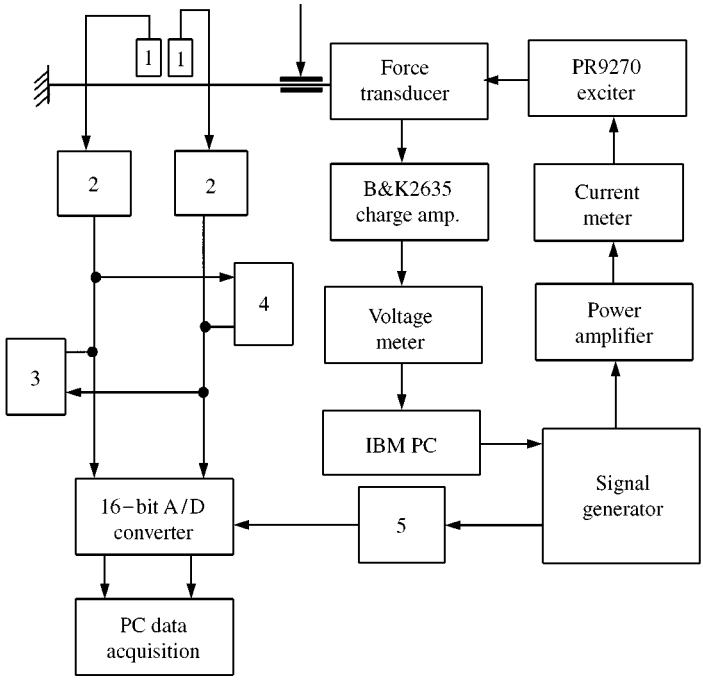

Figure 2. A sketch of the experimental set-up. Note: Accelerometers—1, B&K2635 charge amplifier—2, digital oscilloscope—3, cassette recorder—4, Poincare map pulse generator—5.

found by performing parameter-identification studies and were shown to be very small, so the linear resonance frequencies should be very close to the linear natural frequencies. In the next two subsections, experimental results are presented for two different forcing regions: near twice the natural frequency where the subharmonic resonance is activated, and near the natural frequency of the first mode where the primary resonance is activated.

4. SUBHARMONIC RESONANCE

The frequency used in this experiment was in the region of subharmonic resonance. Four types of experimental plots were constructed using the measured displacement and velocity. Steady state time histories were constructed by high-speed sampling of the displacement at a fixed sampling frequency. Phase diagrams were obtained by plotting discrete values of velocity versus displacement. Fourier spectra of the displacement responses were obtained directly using the fast Fourier transform algorithm. Poincare plots were generated by plotting discrete values of velocity versus displacement.

An excitation frequency was chosen and kept constant, then the excitation amplitude was slowly increased in small increments. At each step the actuator acceleration was held constant by the computer-controlled feedback loop. On-line signal analyses were performed to determine the types of vibratory response. The system exhibited periodic motion, period-doubling bifurcations, leading to chaotic motion with a subsequent increase in excitation amplitude.

Figure 3 shows the time history of displacement in the upper part of the figure, and the phase diagram and frequency spectrum in the lower part at an excitation frequency 10·36 Hz. For small values of the excitation amplitude, the system can be seen to exhibit

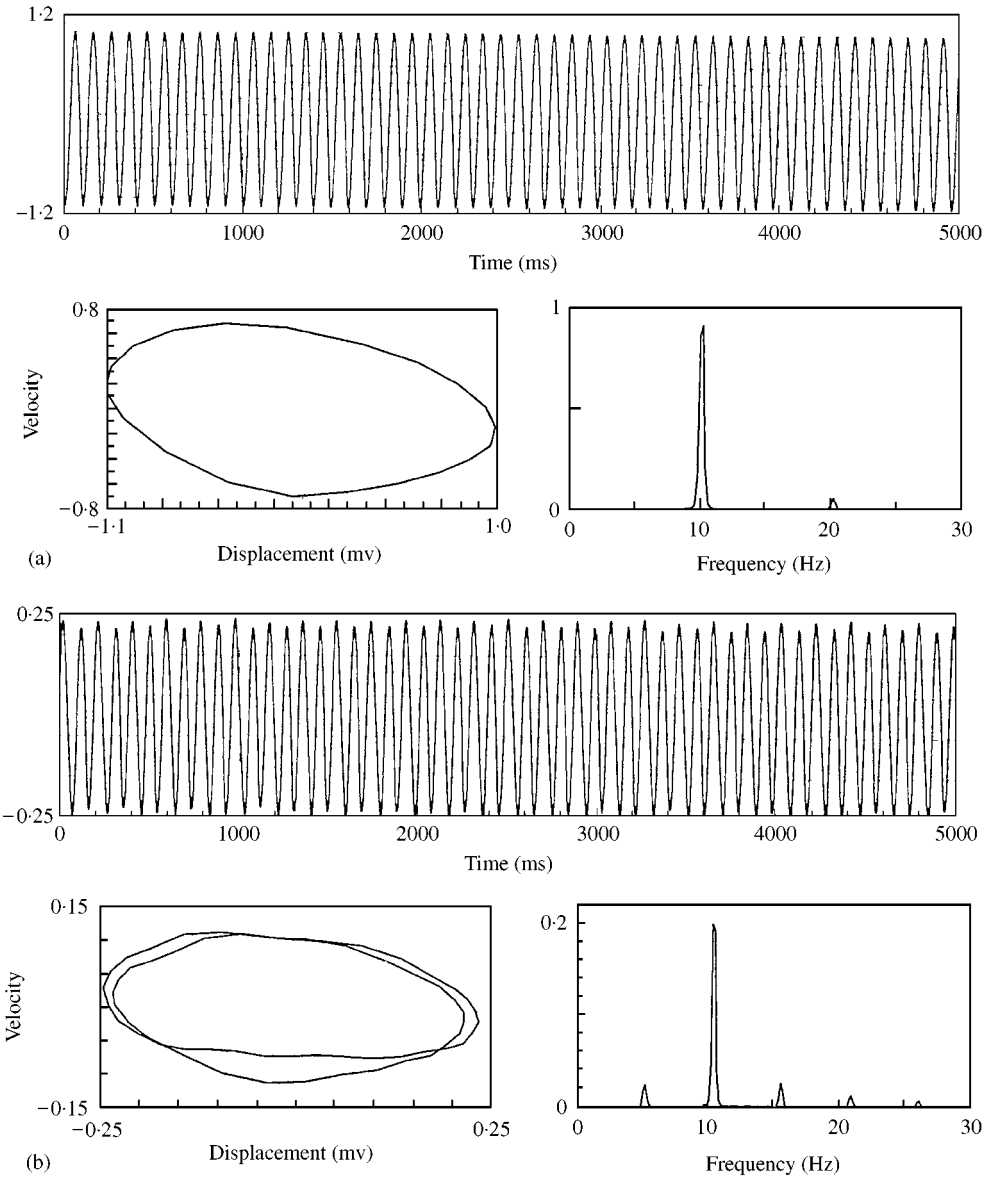

Figure 3. Time histories, accompanying phase-plane diagrams and frequency spectra of the system response for an excitation frequency of 10·36 Hz. Excitation amplitude (a) 0·1, (b) 0·185, (c) 0·19, (d) 0·205, and (e) 0·21 A.

periodic response and the response amplitude is also small. The frequency spectrum for the response shows a linear single frequency motion with very low-level harmonics. Figure 3(a) shows a period-one motion, the phase diagram strengthens this assessment as it shows a closed curve, but its corresponding frequency spectrum shows a higher-frequency component with small value. The amplitude of the response is small.

As the amplitude of excitation increases, both the oval form of the phase diagram and the amplitude of the response grow. By the time the amplitude of excitation reaches 0·185 A, a period-two motion occurs as shown in Figure 3(b). The frequency spectrum now reveals four additional frequency components above and below the excitation frequency

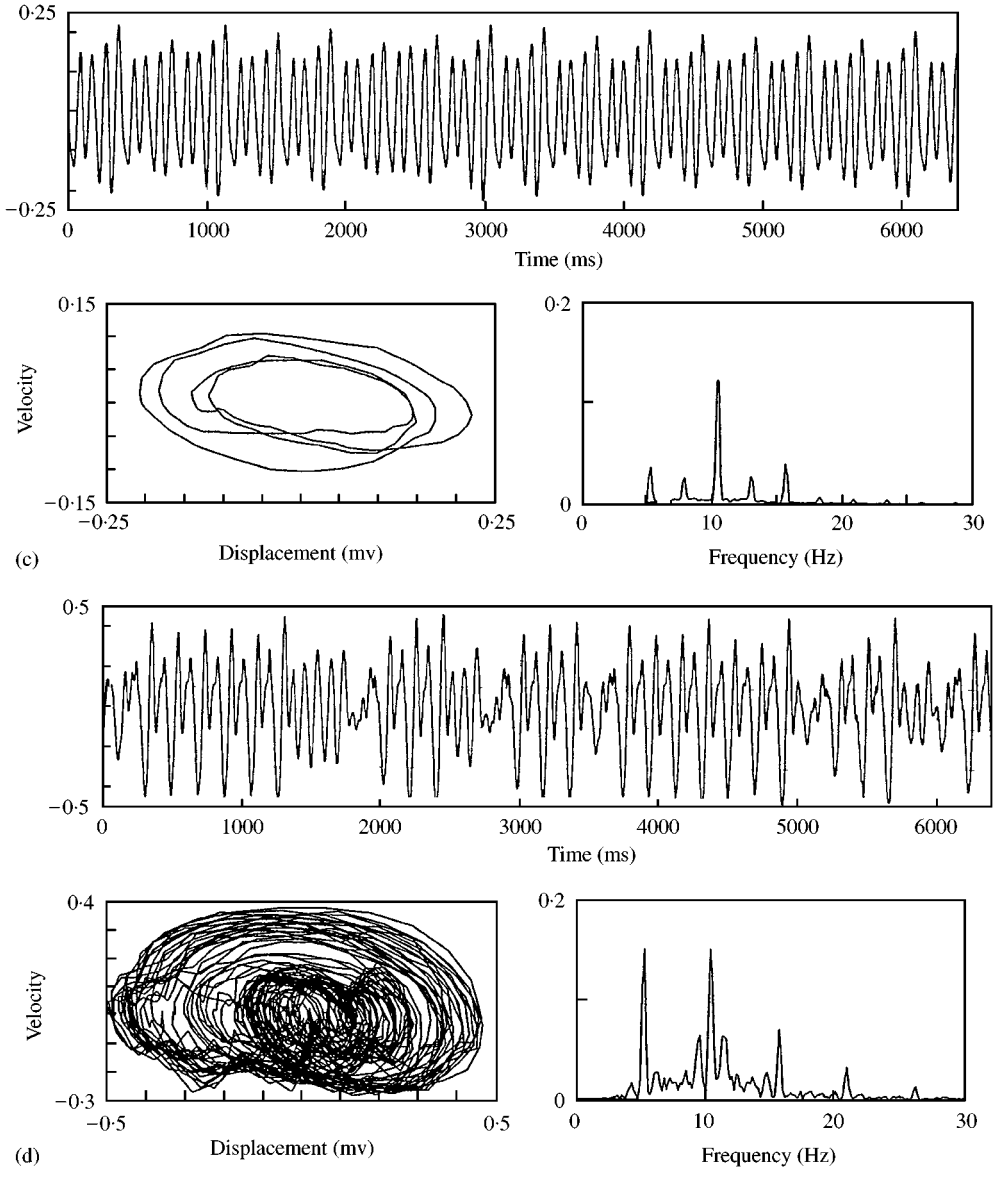

Figure 3. Continued.

corresponding to the 1/2, 3/2, 2, and 5/2 frequency components. The number of closed curves in the phase plane is doubled. As the amplitude of excitation increases slightly to 0·19 A, a period-four motion is observed, as shown in Figure 3(c). The number of closed curves in the phase plane is four-fold. The frequency spectrum shows further sidebands at the 1/4, 3/4, 5/4, and 7/4 components. As the amplitude is increased further, the motion leads to vibrations as shown in Figure 3(d). However, eight-fold closed curves cannot be observed. The reason is that the interval for higher period-doubling motion is very small, and usually cannot be detected when performing mechanical model experiments. A slight broadening of the sideband base is observed in Figure 3(d), which shows some features of chaotic motion. For an amplitude of excitation increase to 0·21 A, the response is shown in

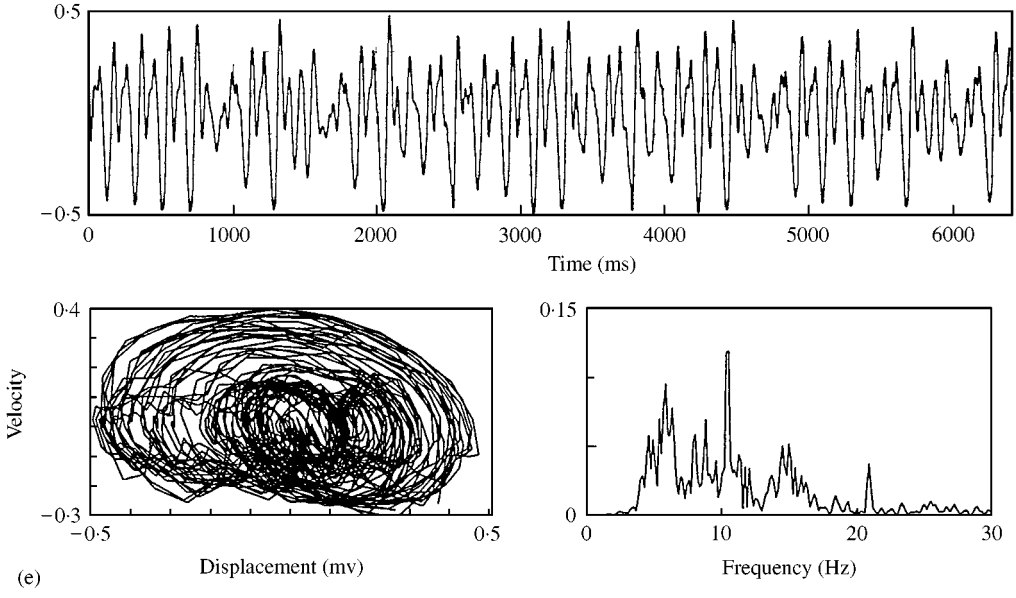

Figure 3. Continued

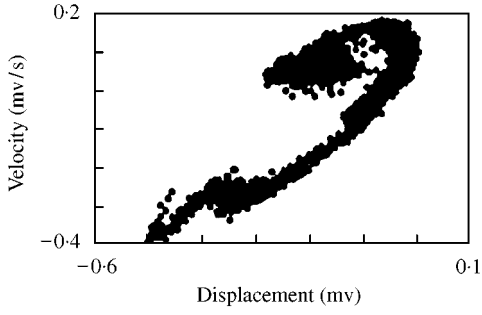

Figure 4. Poincare map for an excitation frequency of 11·44 Hz, and an excitation amplitude of 0·21 A.

Figure 3(e). The unrepeated time series, the strange attractor formed by the Poincare plot and the broadband spectral content of the corresponding Fourier spectrum all suggest that the motion is chaotic [30].

It is noted that the normal bifurcation pattern, a sequence of period-doubling bifurcations leading to chaos (as illustrated in Figure 3), has been commonly observed in the majority of over 20 tests conducted using different system parameters and excitation frequencies, under both the excitation amplitude sweep and excitation frequency sweep.

Figure 4 shows a Poincare section of the trajectory, which is constructed by sampling the motion at the period of the excitation frequency. The figure shows the steady experimental result for 3828 periods after the transient response fully decays. It is clearly a strange attractor.

5. PRIMARY RESONANCE

The normal pattern of a sequence of period-doubling bifurcations leading to chaos was observed near the subharmonic resonance. In this section, the experimental observation of

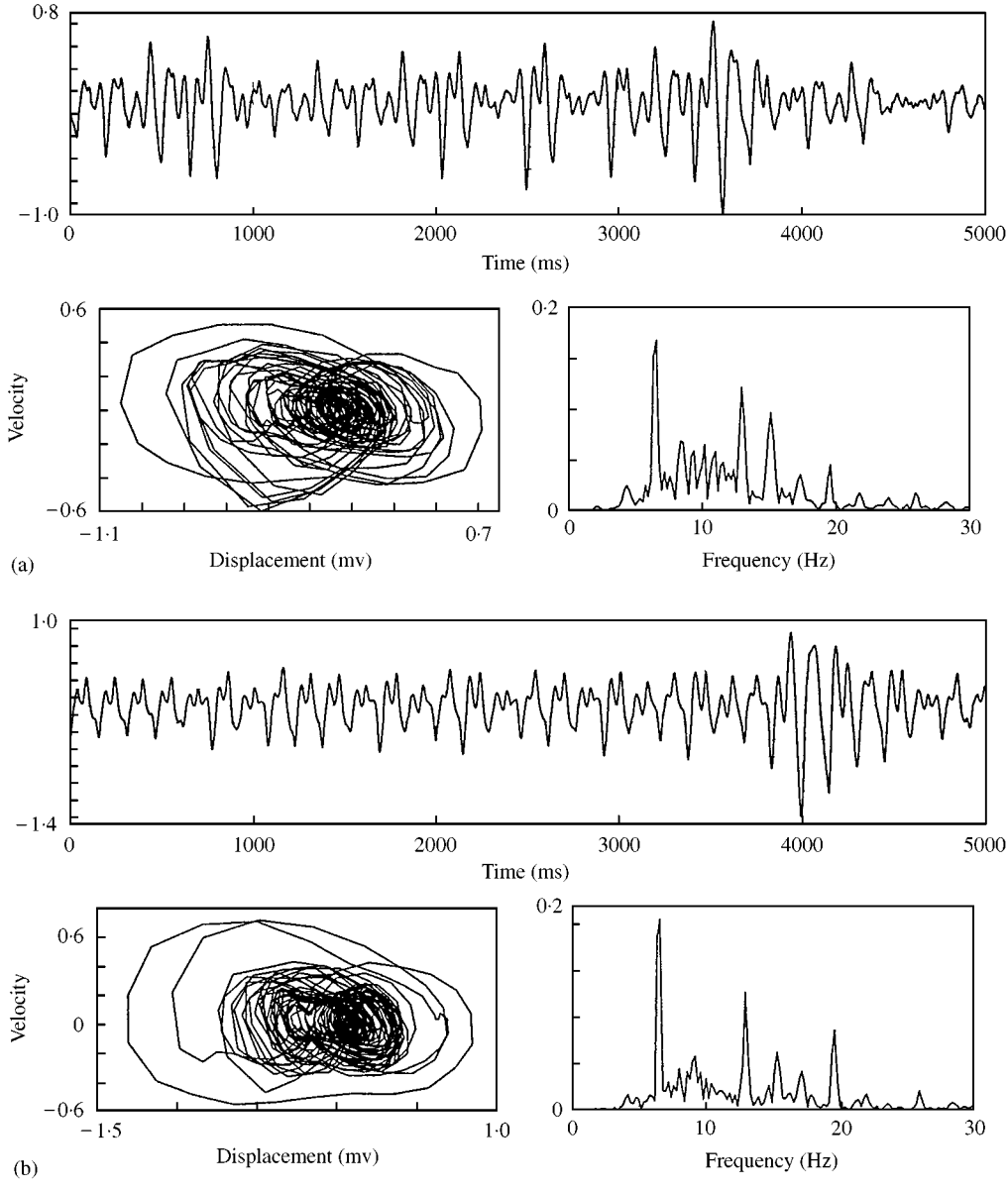

Figure 5. Time histories, accompanying phase-plane diagrams and frequency spectra of the system response for an excitation frequency of 6·6 Hz. Excitation amplitude (a) 877, (b) 980, (c) 1069, (d) 1186, (e) 1209, and (f) 1252 mV.

a window of period-three motion and a reverse period-doubling bifurcation is discussed for an excitation frequency near the primary resonance of the first natural frequency.

Figure 5 shows the partial response of the beam excited at a frequency of 6·6 Hz, as a function of a gradual variation in the excitation amplitude. The responses of the system corresponding to an excitation amplitude below 877 mV are not given for the sake of brevity. Figures 5(a) and 5(b) show chaotic motions of the system at the excitation amplitude 877 and 980 mV, respectively. For an excitation amplitude increase to 1069 mV, the response is shown in Figure 5(c). It is not clear from the phase diagram and the frequency spectrum if the response is multi-periodic or chaotic. By the time the amplitude of

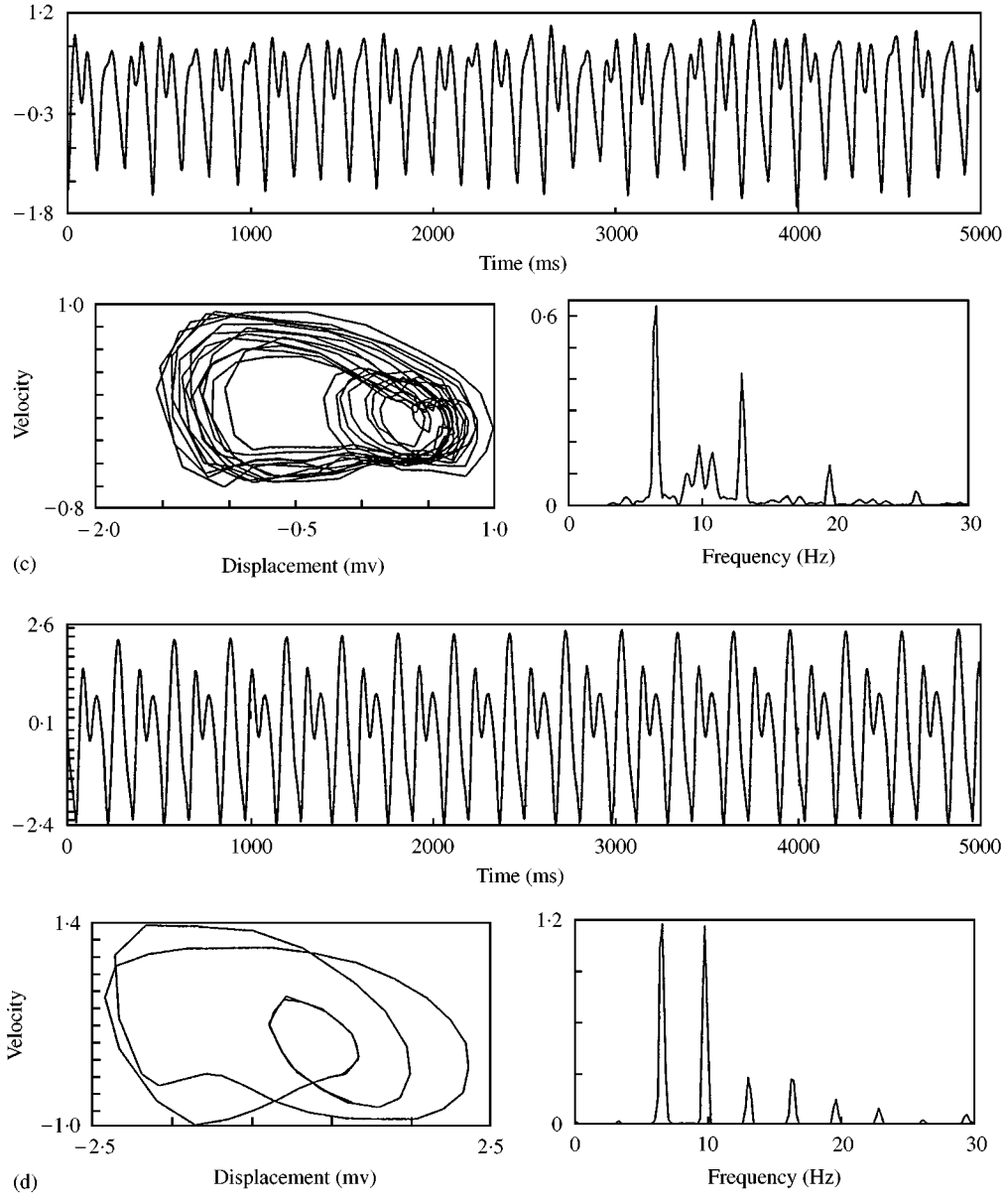

Figure 5. Continued.

excitation reaches 1186 mV, the period-three motion is detected, as shown in Figure 5(d) for which the frequency spectrum indicates many harmonic components. As the amplitude of excitation increases further, chaotic motion is observed again. Thus, it can be concluded that there exists a window of period-three motion between chaotic motions. When the amplitude of excitation is increased to 1252 mV (Figure 5(f)), a period-four motion is detected.

Figure 6 shows a partial sequence of reverse period-doubling bifurcations coming out of chaos as the excitation amplitude increases. Figure 6(a) indicates chaotic motion. When the amplitude of excitation exceeds 1020 mV, chaotic motion does not exist anymore. Instead,

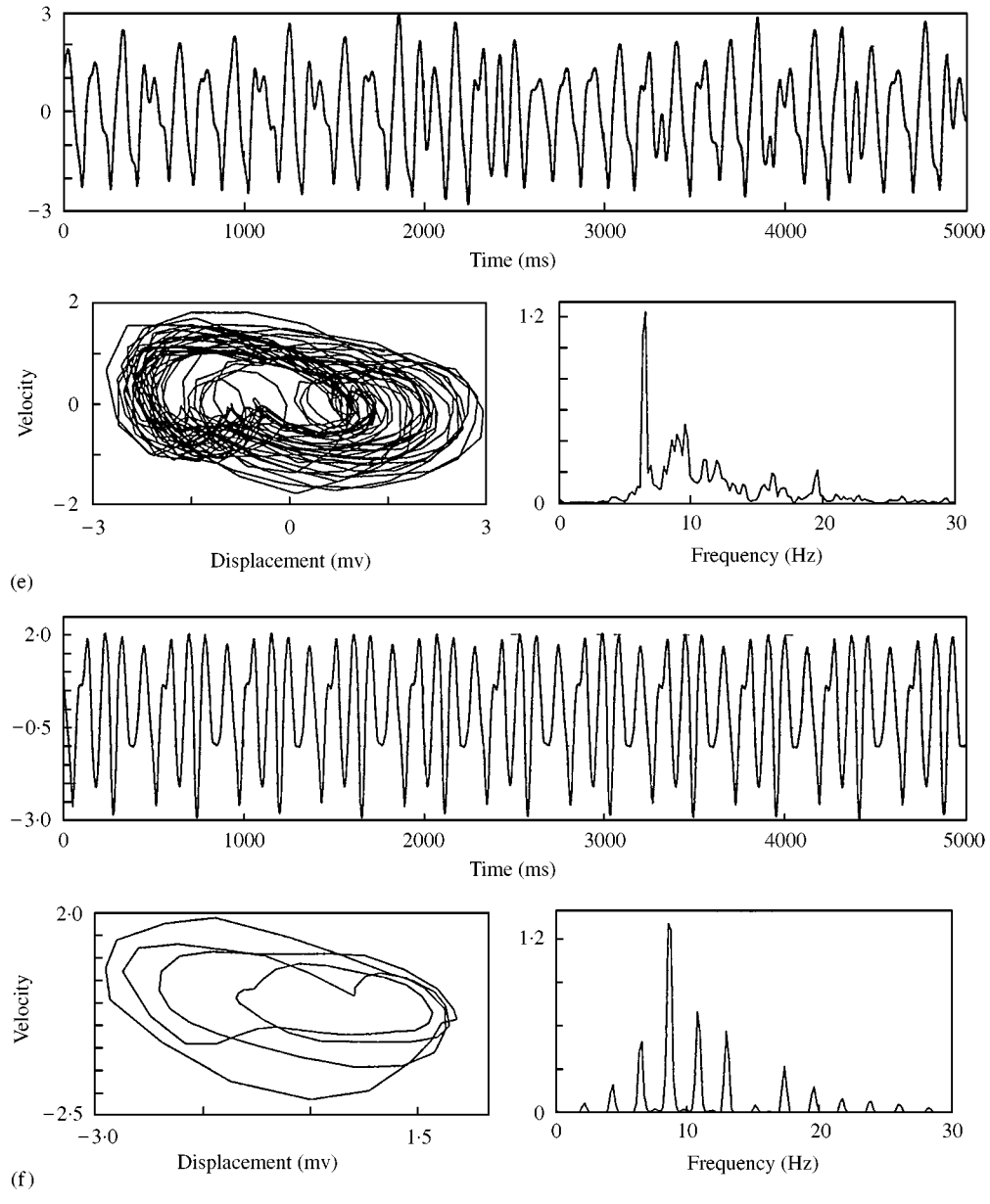

Figure 5. Continued.

period-six motion is observed, corresponding to an amplitude of excitation of 1023 mV (as shown in Figure 6(b)). As the amplitude of excitation increases further, the response of the beam does not follow the normal bifurcation pattern. Instead, a period-demultiplying sequence of bifurcations (from 8 to 4) occurs and is shown in Figures 6c–e. Unfortunately, period-two and period-one motions were not detected since the exciter could not provide enough output to explore such a response.

Near the primary resonance, chaotic motion is usually observed at small amplitudes of excitation. Figure 7 shows a typical Poincare map of chaotic motion.

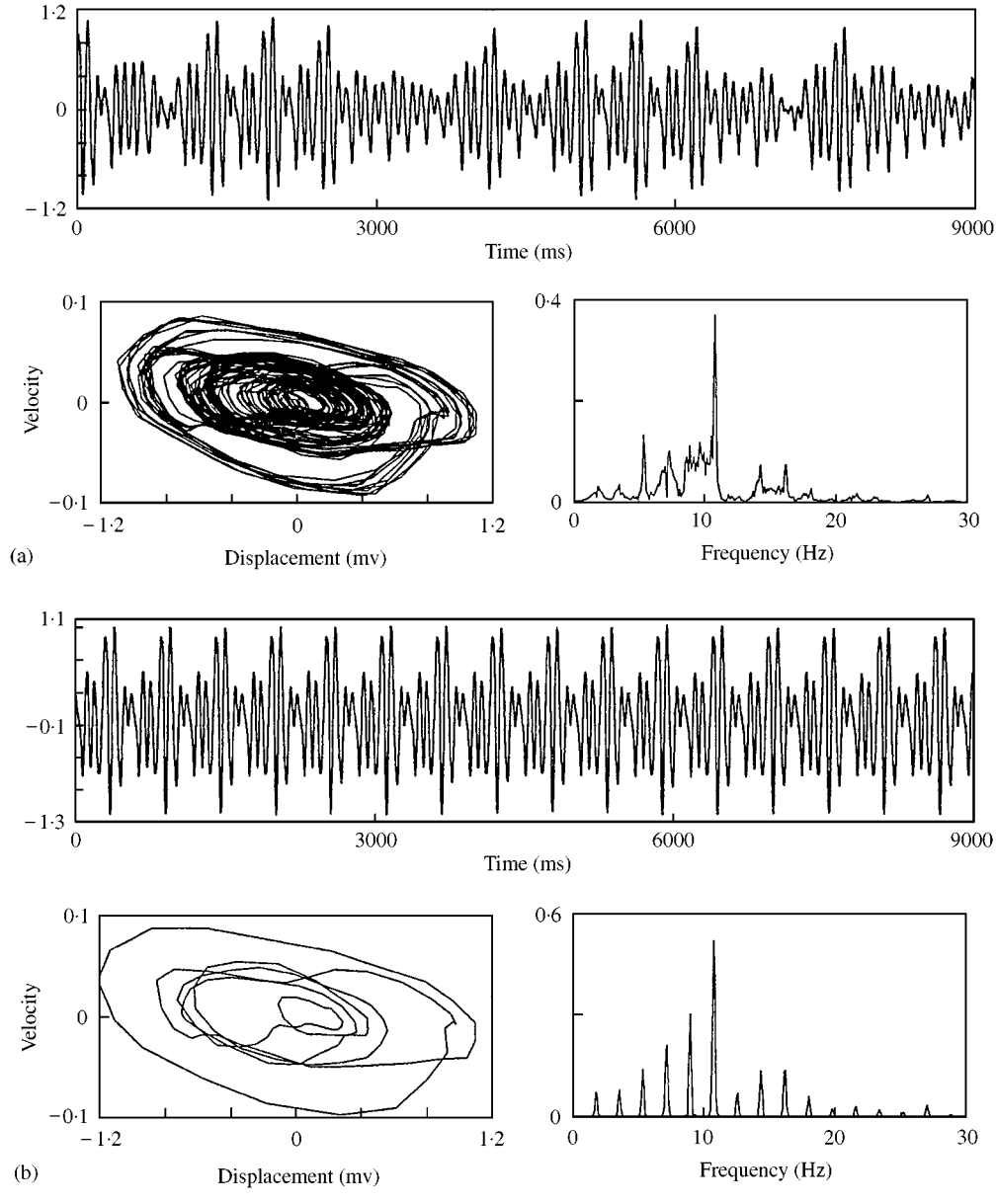

Figure 6. Time histories, accompanying phase-plane diagrams and frequency spectra of the system response for an excitation frequency of 5·5 Hz. Excitation amplitude (a) 1013, (b) 1023, (c) 1035, (d) 1082, (e) 1108, and (f) 1124 mV.

6. EFFECT OF DAMPING ON DYNAMIC INSTABILITY

Parametric resonance may occur over a range of forcing frequencies. Therefore, prediction of the regions of instability in the parameter space becomes critical. Figure 8 shows the experimentally obtained bifurcation diagram on the excitation amplitude–frequency space near a subharmonic resonance. The upper curve represents the boundary of appearance of chaotic motion, whereas the lower curve represents the boundary of occurrence of period-doubling bifurcations.

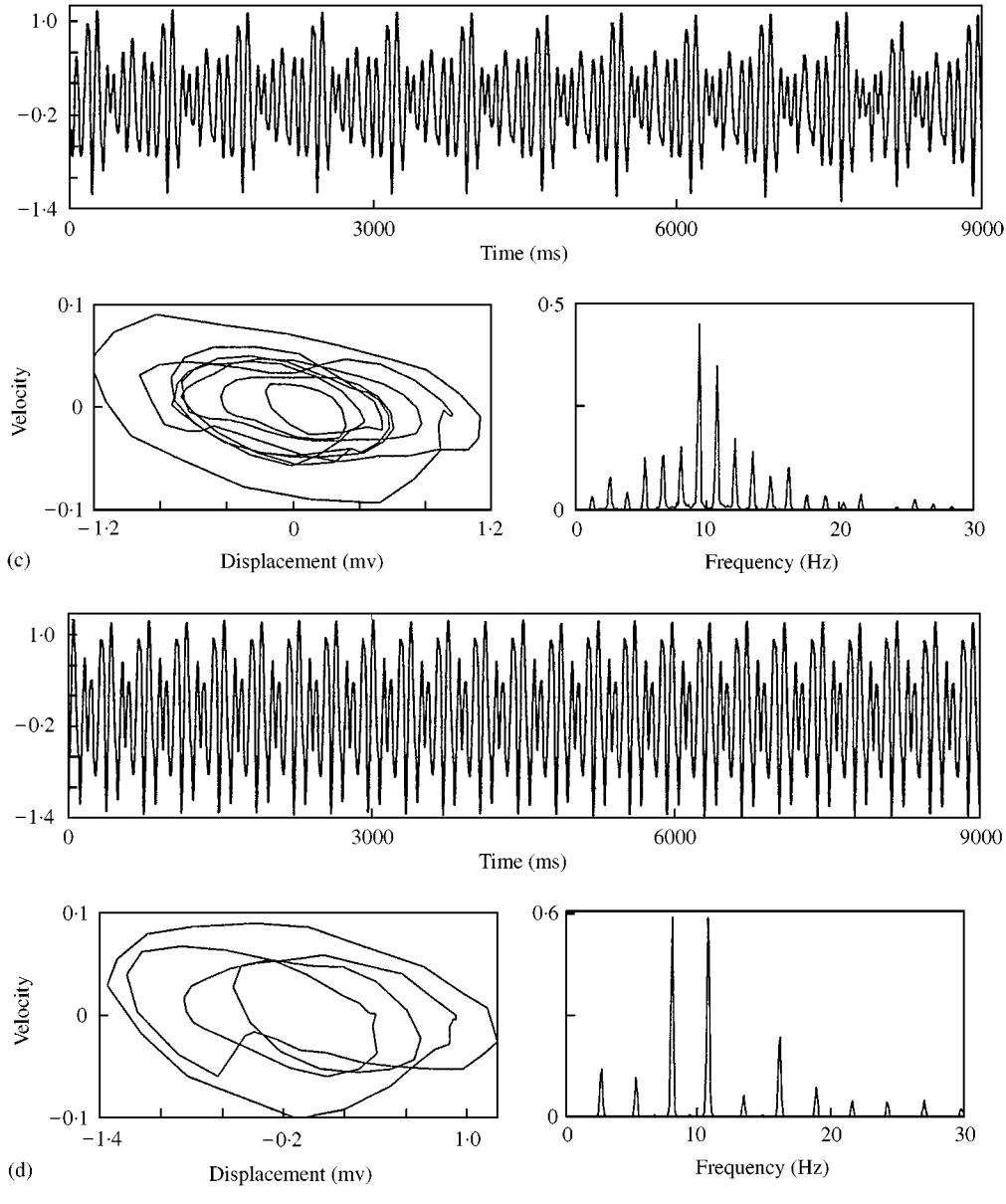

Figure 6. Continued.

As is well known, chaotic motion is very sensitive to initial conditions. The procedure for obtaining the data represented by the curves in Figure 8 was as follows. The experiment was started by selecting an initial excitation frequency and fixing it; then the excitation amplitude was slowly increased in small increments. At each step the excitation output was held constant by the computer-controlled feedback loop. Sufficient time was allowed to elapse so that steady state motion was achieved. The Poincare sections, frequency spectra and phase diagrams were used to ascertain if a response had achieved steady state.

When period-two motion occurred, the excitation amplitude was noted. This threshold value was used to construct the lower curve in Figure 8. As the amplitude of excitation

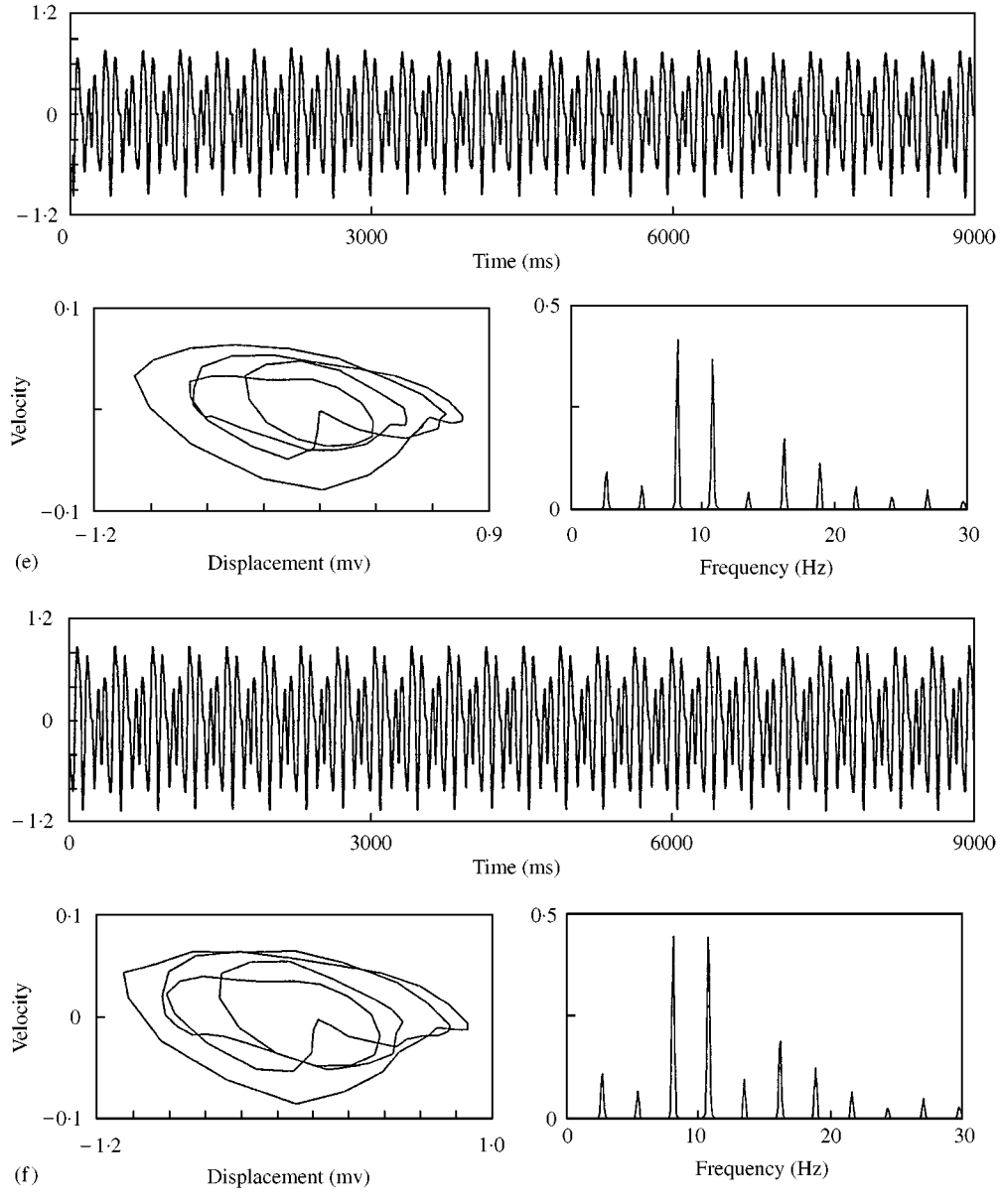

Figure 6. Continued.

increased further, chaotic motion appeared. The critical value for the occurrence of chaos was also noted. Thus, two critical values for this excitation frequency were obtained. The excitation amplitude was then reduced to zero after which the excitation frequency was changed in small increments to another value, and the above procedure repeated. Care was taken to ensure that the small-amplitude increments were properly selected so that a critical value was not bypassed.

The resulting locus of instability of the periodic solutions in the amplitude–frequency parameter space provides valuable information on the overall dynamic behaviour of the system. Qualitative changes can be observed when either the frequency or the amplitude of

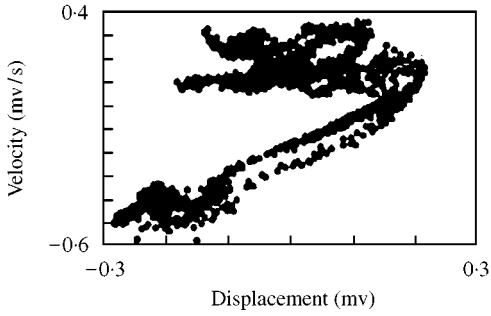

Figure 7. Poincare map for an excitation frequency of 4·5 Hz, and an excitation amplitude of 0.21 A.

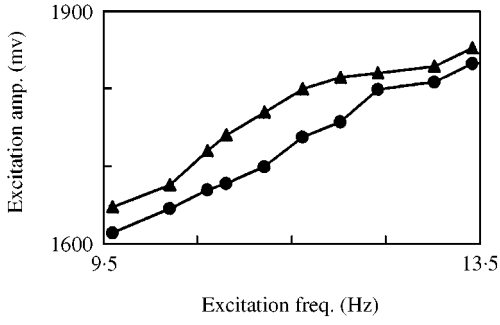

Figure 8. Bifurcation diagram for a normal compressive force 0·5 N.

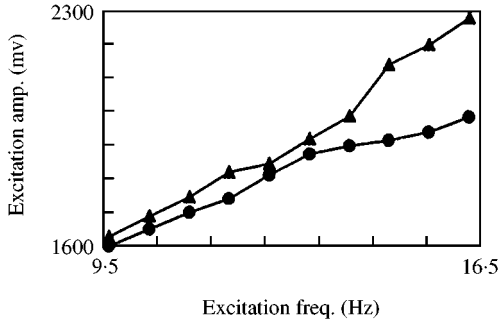

Figure 9. Bifurcation diagram for a normal compressive force 6 N.

excitation is varied across a bifurcation curve. For a fixed frequency, when the excitation level was increased from a very low level, the beam did not respond and remained dynamically stable even with a given manual perturbation. As the amplitude of excitation increased, periodic motion took place across the lower curve, period-doubling bifurcation took place and a stable period-two attractor was obtained. In the narrow region between the two curves a sequence of period-doubling bifurcations is observed. After a few period-multiplications take place a broadband frequency content appears in the FFT across the upper curve, indicating the presence of a chaotic attractor.

If the normal compressive force P_N at the sliding end of the beam was increased, the frictional force increased. Thus, the effects of damping on the dynamic instability were able to be investigated. Figure 9 shows the bifurcation diagram under the larger compressive force P_N. Comparing Figures 8 and 9, one can conclude that the same qualitative results are

obtained for high- as for low-damping levels. The major difference is that the width of the chaotic band in the amplitude of excitation–frequency plane for the low-damping case is much narrower than its counterpart for higher damping. Another difference is that the higher damping case requires a higher amplitude of excitation to show the period-doubling bifurcations leading to chaos.

7. CONCLUSIONS

The non-linear response of a post-buckled beam subject to a parametric excitation was experimentally investigated. Period-doubling bifurcation, period-demultiplying bifurcation, period-three motion and chaotic motions were observed. Increasing and decreasing the normal compressive force at the sliding end of the beam could change the damping of system, allowing the effect of damping on the dynamic stability to be investigated. The experimental bifurcation diagrams were constructed in a similar way to the numerical ones; that is, by varying one of the parameters while the others were kept constant. For sufficiently small values of excitation, the system simply oscillated about the near static equilibrium point and the corresponding amplitudes of oscillation were relatively small. As the amplitude of excitation was increased, the system experienced large-amplitude oscillations and underwent period-doubling bifurcation leading to chaos.

REFERENCES

1. A. H. NAYFEH and D. T. MOOK 1979 *Nonlinear Oscillations*. New York: John Wiley & Sons.
2. W. Y. TSENG and J. DUGUNDJI 1971 *ASME Journal of Applied Mechanics* **38**, 467–476. Nonlinear vibrations of a buckled beam under harmonic excitation.
3. F. C. MOON and P. J. HOLMES 1979 *Journal of Sound and Vibration* **65**, 275–296. A magnetoelastic strange attractor.
4. P. HOLMES and F. C. MOON 1983 *ASME Journal of Applied Mechanics* **50**, 1021–1032. Strange attractors and choas in nonlinear mechanics.
5. F. C. MOON and S. W. SHAW 1983 *International Journal of Non-Linear Mechanics* **18**, 465–477. Chaotic vibrations of a beam with nonlinear boundary conditions.
6. F. MOON and W. T. HOLMES 1985 *Physics Letter A* **111**, 157–160. Double Poincare sections of a quasi-periodically forced, chaotic attractor.
7. N. S. ABHYANKAR, E. K. HALL II and S. V. HANAGUD 1993 *ASME Journal of Applied Mechanics* **60**, 167–174. Chaotic vibrations of beams: numerical solution of partial differential equations.
8. A. M. ABOU-RAYAN, A. H. NAYFEH and D. T. MOOK 1993 *Nonlinear Dynamics* **4**, 499–525. Nonlinear response of a parametrically excited buckled beam.
9. R. A. IBRAHIM 1985 *Parametric Random Vibrations*. New York: John Wiley.
10. G. SCHMIDT and A. TONDL 1986 *Non-Linear Vibrations*. Berlin: Akademi-Verlag.
11. A. K. BAJAJ 1987 *International Journal of Non-linear Mechanics* **22**, 47–59. Bifurcations in a parametrically excited nonlinear oscillator.
12. L. D. ZAVODNEY and A. H. NAYFEH 1988 *Journal of Sound and Vibration* **120**, 63–93. The response of a single-degree-of-freedom system with quadratic and cubic nonlinearities to a fundamental parametric resonance.
13. L. D. ZAVODNEY, A. H. NAYFEH and N. E. SANCHEZ 1989 *Journal of Sound and Vibration* **129**, 417–442. The response of a single degree-of-freedom system with quadratic and cubic nonlinearities to a principal parametric resonance.
14. L. D. ZAVODNEY, A. H. NAYFEH and N. E. SANCHEZ 1990 *Nonlinear Dynamics* **1**, 1–21. Bifurcations and chaos in parametrically excited single-degree-of-freedom system.
15. Y. S. CHEN and L. T. MEI 1990 *Science in China* (*Series A*) **33**, 1469–1476. Bifurcation solutions of general resonant cases of nonlinear Mathieu equation.
16. Y. S. CHEN and K. J. ZHAN 1990 *Applied Mathematics and Mechanics* **11**, 239–245. Some generalization on bifurcation theory of subharmonic resonance in nonlinear Mathieu's equation.

17. Q. S. Lu and C. W. S. To 1991 *Nonlinear Dynamics* **2**, 419–444. Principal resonance of a nonlinear system with two-frequency parametric and self-excitation.
18. Y. S. Chen and J. Xu 1996 *Science in China* (*Series A*) **39**, 405–417. Universal classification of bifurcation solutions to a primary parametric resonance in van der Pol–Duffing–Mathieu's system.
19. Y. S. Chen and J. Xu 1996 *Nonlinear Dynamics* **10**, 203–220. Local bifurcation theory of nonlinear systems with parametric excitation.
20. D. S. Wang and Y. S. Chen 1996 *Journal of Vibration Engineering* **9**, 54–59. The chaos of the nonlinear vibrating system under external and parametric excitation.
21. Y. S. Chen and W. F. Langford 1988 Acta Mechanica Sinica **20**, 522–532. The subharmonic bifurcation solution of nonlinear Mathieu's equation and Euler dynamically buckling problem.
22. S. N. Chow and J. K. Hale 1982 *Methods of Bifurcation Theory*. New York: Springer-Verlag.
23. N. E. Sanchez and A. H. Nayfeh 1990 *International Journal of Non-Linear Mechanics* **25**, 163–176. Prediction of bifurcations in a parametrically excited Duffing oscillator.
24. A. H. Nayfeh, W. Kreider and T. J. Anderson 1995 *AIAA Journal* **33**, 1121–1126. An analytical and experimental investigation of the natural frequencies and mode shapes of buckled beams.
25. L. D. Zavodney and A. H. Nayfeh 1989 *International Journal of Nonlinear Mechanics* **24**, 105–125. The nonlinear response of a slender beam carrying a lumped mass to a principal parametric excitation: theory and experiment.
26. T. J. Anderson, A. H. Nayfeh and B. Balachandran 1996 *ASME Journal of Vibration and Acoustics* **118**, 21–27. Experimental verification of the importance of the nonlinear curvature in the response of a cantilever beam.
27. M. L. Rarmussen 1977 *International Journal of Nonlinear Mechanics* **12**, 81–90. On the damping decrement for nonlinear oscillations.
28. Y. S. Chen, M. Ye and K. J. Zhan 1990 *Journal of Applied Mechanics* **7**, 11–16. Experimental investigation of 1/2 subharmonic bifurcation solution in Mathieu's equation.
29. J. C. Ji and Y. S. Chen 1997 *Journal of Vibration Engineering* **10**, 142–147. An experimental study of instability loci of a parametrically excited nonlinear oscillator.
30. F. C. Moon 1992 *Chaotic and Fractal Dynamics*. New York: John Wiley.